Journal of Power Sources 193 (2009) 570–574

Contents lists available at ScienceDirect

Journal of Power Sources

journal homepage: www.elsevier.com/locate/jpowsour

Short communication

Titanium oxynitride films for a bipolar plate of polymer electrolyte membrane fuel cell prepared by inductively coupled plasma assisted reactive sputtering

S.Y. Kim*, D.H. Han, J.N. Kim, J.J. Lee

Department of Materials Science and Engineering, Seoul National University, Silim 9-dong, Kwanak-gu, Seoul 151-742, South Korea

ARTICLE INFO

Article history:
Received 15 December 2008
Received in revised form 18 March 2009
Accepted 27 March 2009
Available online 23 April 2009

Keywords:
Titanium oxynitride
Bipolar plate
Polymer electrolyte membrane fuel cell
Corrosion
Interfacial contact resistance
Inductively coupled plasma

ABSTRACT

Titanium oxynitride (TiN_xO_y) films are investigated for application as a bipolar plate coating material in a polymer electrolyte membrane fuel cell (PEMFC). TiN_xO_y films with various amounts of oxygen are deposited on stainless-steel substrates by inductively coupled plasma (ICP) assisted reactive sputtering by changing the oxygen gas flow rate. The interfacial contact resistance (ICR) and the corrosion resistance of the TiN_xO_y films are measured under PEMFC simulated conditions. When the amount of oxygen in the TiN_xO_y film is approximately <12 at.% (O_2 flow rate ≤0.2 sccm), the corrosion resistance is enhanced considerably, whereas the interfacial contact resistance does not change. The corrosion current density decreases from 8×10^{-6} A cm^{-2} for the TiN-coated sample to 2.7×10^{-6} A cm^{-2} at 0.6 V vs. SCE as a result of oxygen incorporation in the TiN film. The ICR value remains at 2.5 mΩ cm^2 at 150 N cm^{-2}. When a small amount of oxygen is added to the TiN film, it is postulated that the oxygen atoms locate at the column and grain boundaries, and thus prevent corrosive media from penetrating into the substrate while not deteriorating the electrical property of the film.

1. Introduction

A polymer electrolyte membrane fuel cell (PEMFC), also known as a proton exchange membrane fuel cell, is a promising type of fuel cell for transportation applications and portable devices. The bipolar plate of the PEMFC performs multiple functions, namely, it conducts electrons to adjoining cells as a current-collector, supports the membrane electrode assembly (MEA), and facilitates the removal of heat and reaction products. Therefore, it needs to have a low contact resistance, a high corrosion resistance, high thermal conductivity, low gas permeability, good mechanical strength, and suitable surface properties for water removal. Stainless-steel is an attractive candidate material for a PEMFC bipolar plate. Nevertheless, an improvement in its material properties, including its corrosion resistance and interfacial contact resistance (ICR), must be made for it to meet the required performance level of a bipolar plate. To improve these properties, various types of coating materials have been applied in an effort to form a protective layer, or layers, on the metal surface. A titanium nitride film is a promising material due to its low electrical resistance and high corrosion resistance. There have been several reports pertaining to investigation of the corrosion behavior of TiN-coated 316L stainless-steel [1–7]. Although the corrosion resistance of TiN-coated 316L stainless-steel has been increased significantly, it is still not recommended for use as a bipolar plate.

This study attempts to enhance the corrosion resistance of a TiN-coated stainless-steel substrate by adding a small amount of oxygen to the TiN coating. TiN_xO_y films have been investigated for application as a diffusion barrier, as a decorative coating, and for solar panels [8–13]. Most investigations have been carried out on films with very high oxygen contents, and there are no reports concerning the properties of TiN_xO_y film as they relate to a bipolar plate application. Given that oxygen can increase significantly the electrical resistance, the change in the interfacial contact resistance (ICR) by the incorporation of oxygen in the TiN_xO_y coatings has also been investigated.

2. Experimental details

TiN_xO_y films were deposited on stainless-steel 316L (SS 316L) substrates by inductively coupled plasma (ICP) assisted sputtering. The ICP power was generated by applying an RF power of 13.56 MHz through a tuning network to a coil installed in the chamber. The power was held constant at 400 W. The target d.c. power was 400 W (8.77 W cm^{-2}). Before the deposition, the substrate was cleaned in ultrasonic baths of acetone and ethanol for 20 min, each. The chamber was evacuated to $<5 \times 10^{-7}$ Torr using a turbo molecular pump, and the deposition was carried out at a constant total pressure of 10 mTorr in a gas mixture of Ar, N_2 and O_2. The oxygen flow rate was varied from 0 to 0.8 sccm. A titanium target with a

* Corresponding author. Tel.: +82 2 880 5511; fax: +82 2 871 5540.
E-mail address: neo0706@naver.com (S.Y. Kim).

0378-7753/$ – see front matter © 2009 Elsevier B.V. All rights reserved.
doi:10.1016/j.jpowsour.2009.03.076

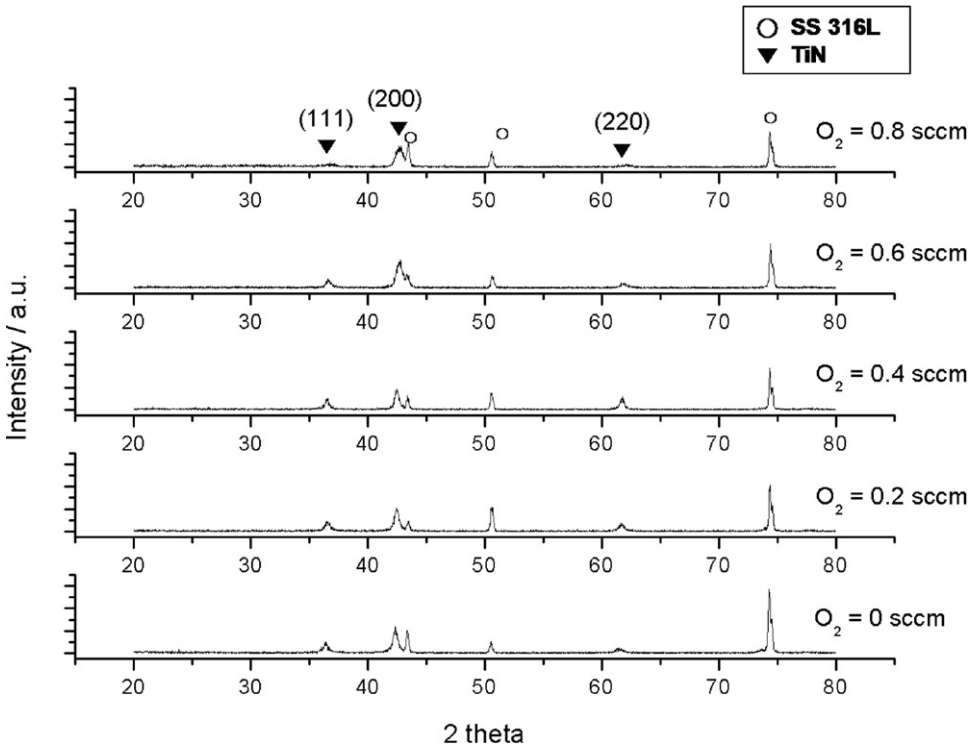

Fig. 1. XRD diffraction patterns of TiN_xO_y films on SS 316L substrate as a function of O_2 flow rate.

diameter of 3 in. at a purity of 99.995% (CERAC) was used. During the deposition, the substrate temperature was maintained at 400 °C. To obtain films with similar thicknesses, the deposition time was varied between 30 and 60 min, since the deposition rate decreased as the oxygen flow rate increased due to a target poisoning effect.

For ICR measurements, the TiN_xO_y films were coated on both sides of the substrate. The microstructure and composition of the TiN_xO_y films were characterized by X-ray diffraction (XRD, MAC Science M18XHF-SRA), auger electron spectroscopy (AES, Perkin-Elmer model 660) and field emission scanning electron microscopy (FESEM, JEOL JSM-6330F).

The Davies method [14] was used for the ICR measurement. The ICR was evaluated (IM6 from JAHNER electric) under compressive forces up to 150 N cm^{-2}. The ICR value was determined by subtracting the resistance of carbon papers placed between two gold-plated current-collectors from the total resistance [15].

The corrosion resistance was determined by the electrochemical polarization method using an electrochemical analyzer system (VERSASTAT3 from AMTEC). An aqueous solution of 0.1N

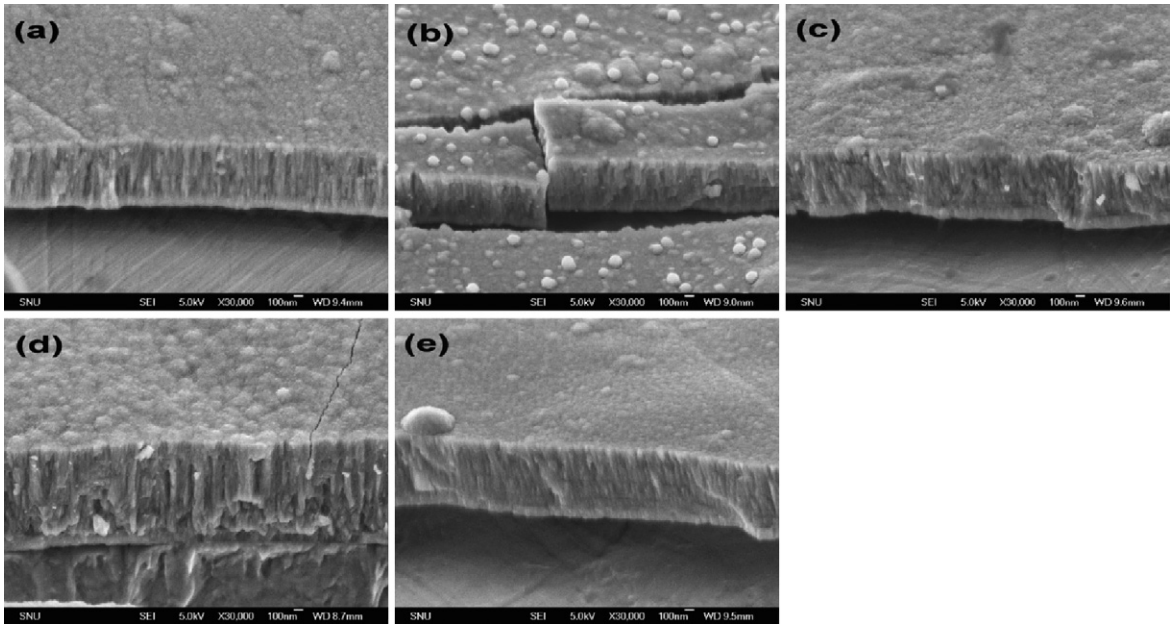

Fig. 2. FESEM images of TiN_xO_y films at different oxygen flow rates on SS 316L; (a) O_2 = 0 sccm, (b) O_2 = 0.2 sccm, (c) O_2 = 0.4 sccm, (d) O_2 = 0.6 sccm, (e) O_2 = 0.8 sccm.

H_2SO_4 + 2 ppm HF served as the electrolyte at a temperature of 80 °C to simulate PEMFC operation conditions. The electrolyte was bubbled either with hydrogen gas for the anode condition or with air for the cathode condition. A conventional three-electrode system was used, in which the working electrode was located in the center of the cell. Additionally, a pair of auxiliary electrodes was located on both sides for better current distribution. The reference electrode was a saturated calomel electrode (SCE). For the potentiodynamic polarization test, the potential scan was changed from −0.6 to 1.0 V vs. the OCP (open circuit potential) at a scan rate of 1.5 mV s^{-1}. Potentiostatic polarization measurements were carried out for 6000 s at −0.1 V for the anode and 0.6 V for the cathode environment.

3. Results and discussion

3.1. Phase composition and microstructure of TiN_xO_y films

Fig. 1 shows the XRD peaks of TiN_xO_y films deposited on a SS 316L substrate at various oxygen flow rates. It is noticed that only TiN peaks are present; does no oxide peaks, such as for TiO_2, were detected. Furthermore, the position of the TiN peaks does not change with oxygen incorporation, which indicates that the TiN lattice parameters remain constant. When a ternary compound is formed and has a crystal structure identical to that of the binary compounds, an XRD peak shift is typically observed [15,16].

FESEM images of TiN_xO_y films deposited at various oxygen flow rates are presented in Fig. 2. The TiN_xO_y film also shows the columnar structure of a typical TiN film. After deposition for 30 min, the thickness of the film is 0.7 μm at 0–0.2 sccm O_2. It decreases to 0.3 μm at 0.4–0.8 sccm O_2. The decrease in the deposition rate is related to a target poisoning effect, as previously mentioned.

Auger concentration depth profiles of TiN_xO_y films deposited at various oxygen flow rates are presented in Fig. 3. The oxygen content in the film and at the surface of the coatings increases as the oxygen flow rate increased. The oxygen content in the matrix increased from 3.5 to 41 at.%, and the oxygen content at the surface increases from 43 to 57.5 at.% as the oxygen flow rate is increased.

3.2. Electrical properties of TiN_xO_y films

The ICR values of TiN_xO_y films deposited at various oxygen flow rates at 150 N cm^{-2} are shown in Fig. 4. The ICR value of the TiN-coated sample is 2.5 mΩ cm^2, and it does not increase at oxy-

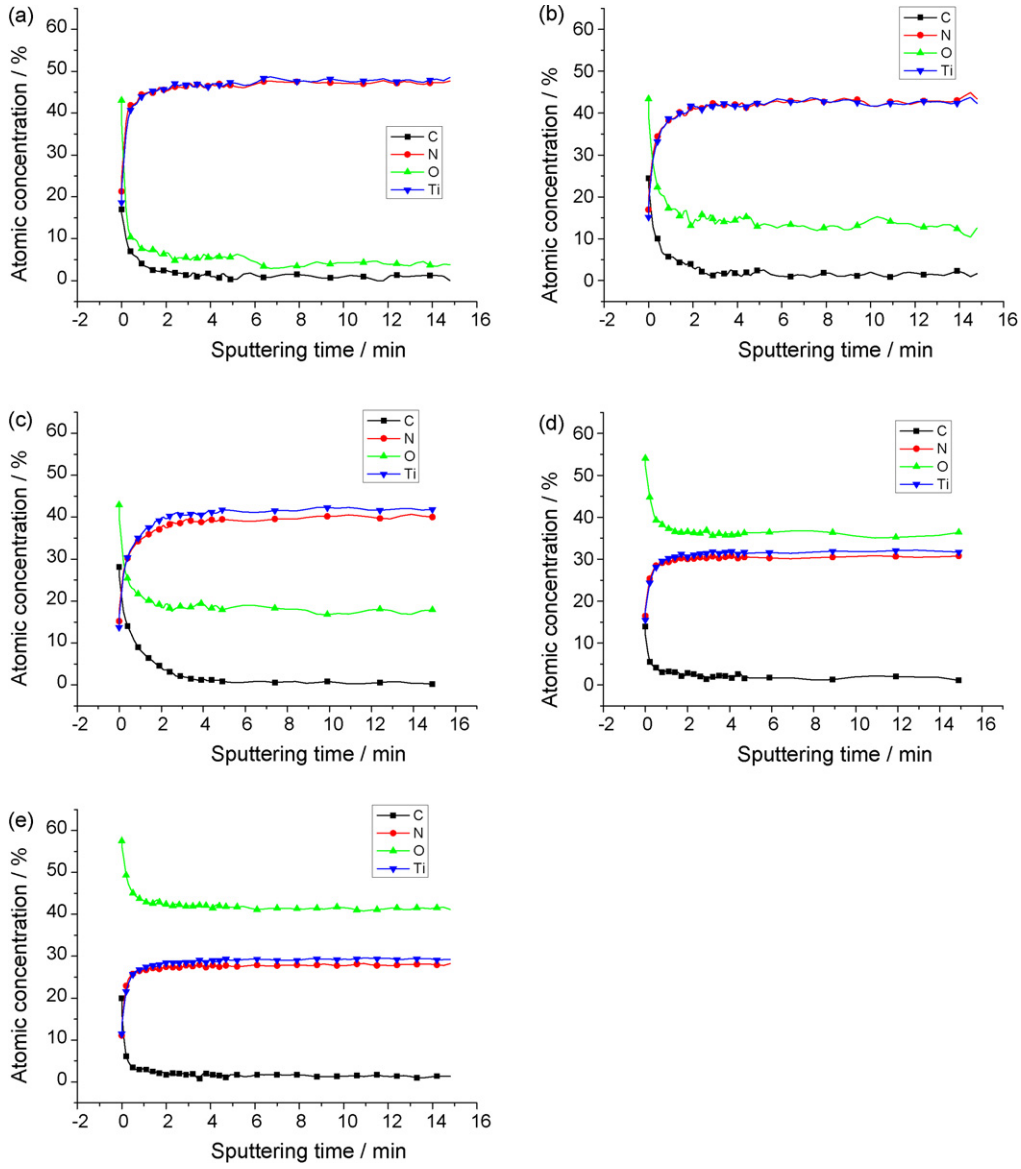

Fig. 3. Auger concentration depth profile of TiN_xO_y films as function of oxygen flow rate: (a) O_2 = 0 sccm, (b) O_2 = 0.2 sccm, (c) O_2 = 0.4 sccm, (d) O_2 = 0.6 sccm, (e) O_2 = 0.8 sccm.

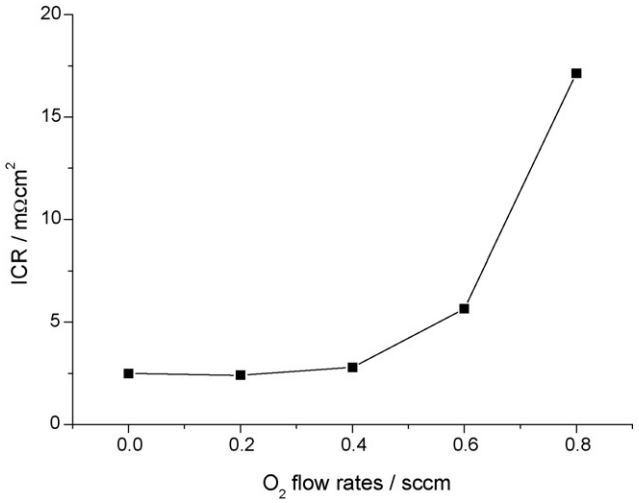

Fig. 4. The ICR of TiN_xO_y films as a function of oxygen flow rate.

gen flow rates up to 0.4 sccm. At >0.6 sccm O_2, however, the ICR increases significantly.

3.3. Corrosion properties of TiN_xO_y films

Fig. 5 shows potentiodynamic polarization curves for uncoated and coated SS 316L samples in an aqueous solution of 0.1 M H_2SO_4 + 2 ppm HF bubbled with (a) air or (b) hydrogen gas at 80 °C. All of the coated samples exhibited higher corrosion resistance compared with the uncoated SS 316L. In particular, TiN_xO_y deposited at 0.2 sccm O_2 has the highest corrosion resistance under cathode and anode conditions. The corrosion current density of this sample is 2.7×10^{-6} A cm^{-2} at 0.6 V vs. SCE in the cathode condition, whereas that of the TiN-coated sample is 8×10^{-6} A cm^{-2} at the same potential. The corrosion potential also increases considerably for the TiN_xO_y sample. The samples show different corrosion potentials at different oxygen concentrations. This feature is attribute to different forms of pitting corrosion. Different corrosion potential values have also been observed in (Ti,Cr)N-coated samples with different nitrogen concentrations [15].

The results from the potentiostatic polarization measurements are presented in Fig. 6. In the cathode condition (Fig. 6(a)), all of the TiN_xO_y film samples stabilize at a low current density at approximately 2×10^{-6} A cm^{-2}. In the anode condition (Fig. 6(b)), the TiN_xO_y-coated samples deposited at <0.4 sccm O_2 have negative current densities as they have corrosion potentials that are greater than −0.1 V, which implies that the TiN_xO_y films act as a cathodic protection material. On the other hand, a positive current is observed with the TiN_xO_y-coated samples at high oxygen flow rates (>0.6 sccm).

It is assumed that at low oxygen flow rates, most oxygen atoms do not replace nitrogen in the TiN matrix. Instead, they are located at the column and grain boundaries, as suggested by the XRD peak position in Fig. 2. Nicolett and sinke [17–19] also argued that the enhanced diffusion barrier property of TiN_xO_y film compared with that of TiN film is caused by the blocking effect of oxygen. The diffusion paths along defects are blocked by oxygen in the TiN_xO_y-coated

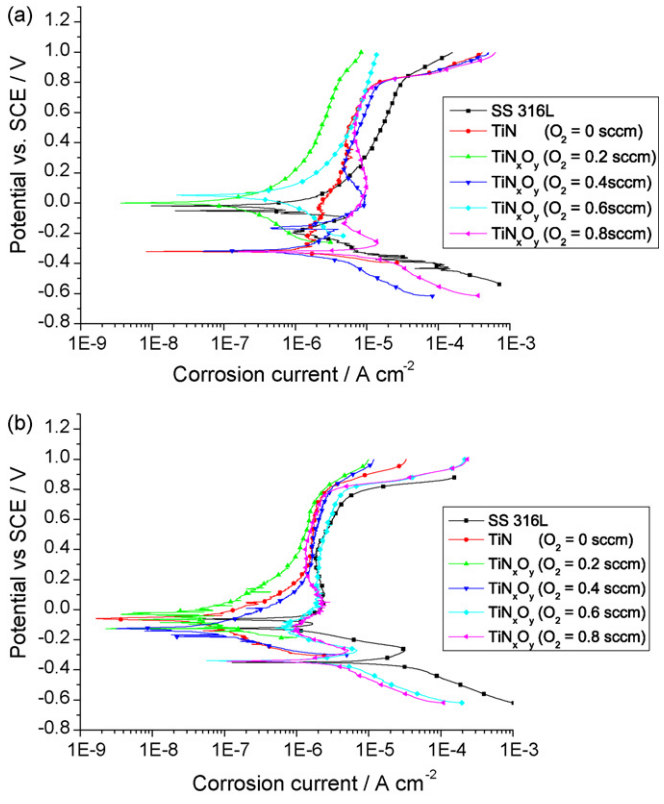

Fig. 5. Potentiodynamic curves of TiN_xO_y films under (a) the cathode (air bubbling) and (b) anode (hydrogen bubbling) conditions.

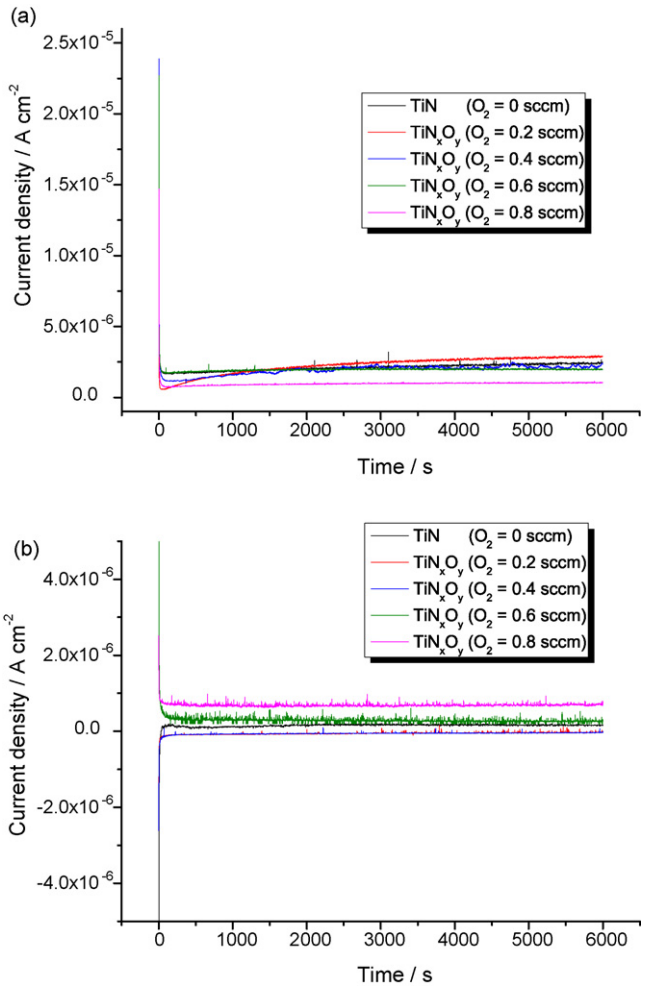

Fig. 6. Potentiostatic curves of TiN_xO_y films under (a) the cathode (0.6 V, air bubbling) and (b) anode (−0.1 V, hydrogen bubbling) conditions.

sample. Park et al. [20] also reported from a TEM investigation that oxygen can be easily trapped at the porous spaces between columnar TiN grains.

4. Conclusions

TiN_xO_y films with various amounts of oxygen have been deposited on stainless-steel 316L substrates by inductively coupled plasma (ICP) assisted reactive sputtering at different oxygen gas flow rates. The corrosion resistance of the film is increased significantly by introducing a small amount of oxygen (<12 at.%) into the TiN film, whereas the ICR value does not increase. With a corrosion current density of 2.7×10^{-6} A cm^{-2} at 0.6 V vs. SCE and an ICR value of 2.5 mΩ cm^2 at 150 N cm^{-2}, the TiN_xO_y film can be regarded as a potential alternative to the TiN film as a coating material for a PEMFC bipolar plate. Oxygen atoms are likely located at the column and the grain boundaries, and thereby prevent corrosive media from penetrating into the substrate while not deteriorating the electrical property of the film.

Acknowledgement

The financial support, provided by the Fundamental R&D program for Core Technology of Materials (M-2007-01-0006) funded by the Ministry of Commerce, Industry and Energy (MOCIE), Republic of Korea, is greatly appreciated.

References

[1] P. Bhardwaj, O.J. Gregory, K. Bragga, M.H. Richman, Appl. Surf. Sci. 48/49 (1991) 555–566.
[2] M. Li, S. Luo, C. Zeng, J. Shen, H. Lin, C. Cao, Corros. Sci. 46 (2004) 1369–1380.
[3] E.A. Cho, U.S. Jeon, S.A. Hong, I.H. Oh, S.G. Kang, J. Power Sources 142 (2005) 177–183.
[4] L. Chenglong, Y. Dazhi, L. Guoqiang, Q. Min, Mater. Lett. 59 (2005) 3813–3819.
[5] M. Flores, L. Huerta, R. Escamilla, E. Andrade, S. Muhl, Appl. Surf. Sci. 253 (2007) 7192–7196.
[6] Y. Wang, D.O. Northwood, J. Power Sources 165 (2007) 293–298.
[7] B. Subramanian, M. Jayachandran, Mater. Lett. 62 (2008) 1727–1730.
[8] N. Kumar, M.G. Fissel, K. Pourrezaei, B. Lee, E.C. Douglas, Thin Solid Films 153 (1987) 287–301.
[9] M.H. Kazemeini, A.A. Berezin, N. Fukuhara, Thin Solid Films 372 (2000) 70–77.
[10] A. Alberti, S. Molinaro, F. La Via, C. Bongiorno, G. Ceriola, S. Ravesi, Microelectron. Eng. 60 (2002) 81–87.
[11] F. Vaz, P. Cerqueira, L. Rebouta, S.M.C. Nascimento, E. Alves, Ph. Goudeau, J.P. Rivière, Surf. Coat. Technol. 174–175 (2003) 197–203.
[12] F. Vaz, P. Cerqueira, L. Rebouta, S.M.C. Nascimento, E. Alves, Ph. Goudeau, J.P. Riviere, K. Pischow, J. De Rijk, Thin Solid Films 447–448 (2004) 449–454.
[13] M.-C. Lin, L.-S. Chang, H.C. Lin, Appl. Surf. Sci. 254 (2008) 3509–3516.
[14] D.P. Davies, P.L. Adcock, M. Turpin, S.J. Rowen, J. Appl. Electrochem. 30 (2000) 101–105.
[15] H.S. Choi, D.H. Han, W.H. Hong, J.J. Lee, J. Power Sources 189 (2009) 966–971.
[16] St. Collard, H. Kupfer, G. Hecht, W. Hoyer, H. Moussaoui, Surf. Coat. Technol. 112 (1999) 181–184.
[17] M.A. Nicolet, Thin Solid Films 52 (1978) 415–443.
[18] M.A. Nicolet, M. Bartur, J. Vac. Sci. Technol. 19 (1981) 786–793.
[19] W. Sinke, G.P.A. Frijlink, F.W. Saris, Appl. Phys. Lett. 47 (1985) 471–473.
[20] K.-C. Park, K.-B. Kim, I. Raaijmakers, K. Ngan, J. Appl. Phys. 80 (1996) 5674–5681.